






 Cite this: *Chem. Commun.*, 2021, 57, 10218

 Received 8th August 2021,
Accepted 8th September 2021

DOI: 10.1039/d1cc04336f

rsc.li/chemcomm

Introduction of a $(\text{Ph}_3\text{P})_2\text{Pt}$ group into the rim of an open-cage fullerene by breaking a carbon–carbon bond†

 Steven R. Gralinski, Mrittika Roy,  Lilia M. Baldauf,  Marilyn M. Olmstead  and Alan L. Balch *

Treatment of an open-cage fullerene, designated as MMK-9, with $(\text{Ph}_3\text{P})_4\text{Pt}$ in toluene solution at room temperature allows a $(\text{PPh}_3)_2\text{Pt}$ unit to be incorporated into the rim of the cage so that it becomes an integral part of the carbon cage skeleton. The structure of the adduct has been determined by single crystal X-ray diffraction and reveals that the platinum atom has planar PtC_2P_2 coordination, rather than the usual η^2 -bonding to an intact C–C double bond of the fullerene.

Fullerenes such as C_{60} are closed shell, nearly spherical molecules with a chemically accessible outer surface and a protected interior.¹ By functionalizing and chemically cleaving selected C–C bonds in a fullerene, it is possible to create openings that make it feasible for small molecules to enter the interior of the fullerene.² Many such open-cage fullerenes have been synthesized and used as hosts for small molecules such as H_2 , H_2O , HF, HCHO and HCN.^{2–6} Fullerenes containing metal ions or complexes encapsulated inside of them, known as endohedral metallofullerenes, have to date only been synthesized using the gas phase Krätschmer–Huffman carbon arc process in small yields, requiring arduous separation techniques for isolation.^{7–9} A synthetic pathway utilizing molecular surgery to generate an open-cage compound followed by metal insertion would be a more viable alternative for bulk production of endohedral metallofullerenes.^{6–8} These endohedral metallofullerenes possess magnetic and nuclear properties arising from the nature of the encapsulated metal ions that make them candidates for medical applications such as magnetic resonance imaging (MRI) contrast or diagnostic agents.^{10–12} Although metal ions have not yet been introduced into the interior of open-cage fullerenes, there have been several reports

of the binding of metal complexes to open-cage fullerenes through nitrogen or oxygen donor atoms added to the fullerene during the cage opening process.^{13,14} Here we investigate an approach to adding a metal complex to the rim of an open cage fullerene. The creation of such a compound can offer a means of eventually placing the metal inside the fullerene or the creation of a heterofullerene by incorporating that metal atom into the fabric of an intact fullerene cage. To achieve this end, we have chosen to use a low-valent, soft metal center to avoid binding to hard nitrogen or oxygen donors on the cage opening. We have also taken advantage of the investigations conducted by Rabideau and coworkers involving reactions of semibuckminsterfullerene ($\text{C}_{30}\text{H}_{12}$) and metal complexes that have contributed to the understanding of the interactions between metal atoms and fullerene-like curved π systems.¹⁵

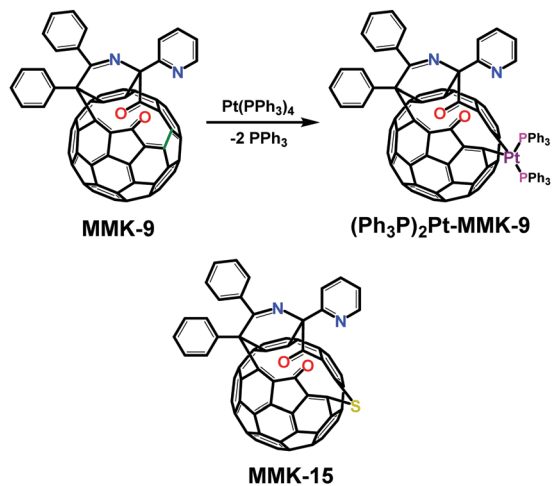
We examine the reactivity of an open-cage fullerene, MMK-9, that has a twelve-membered ring opening on its surface.¹⁶ (We use the authors' initials, MMK, followed by the number used in ref. 14 as names for the compounds involved in this study.) MMK-9 has previously been shown to react with simple transition metal compounds to form ruthenium and silver complexes, often accompanied by unpredictable modification of the fullerene.^{14,17} In order to avoid interactions with the carbonyl and imine functions on this open-cage fullerene, we investigated addition of the low-valent platinum(0) complex, $(\text{Ph}_3\text{P})_4\text{Pt}$, which is known to dissociate triphenylphosphine ligands and to bind with olefins.²⁰ As shown in Scheme 1, treatment of MMK-9 with $(\text{Ph}_3\text{P})_4\text{Pt}$ in dioxygen-free toluene resulted in an immediate color change of the solution from yellow to deep brown. After stirring for 90 min followed by column chromatography on silica gel, $(\text{Ph}_3\text{P})_2\text{Pt}$ -MMK-9 (**1**) was obtained in 46% yield.

Red crystalline plates suitable for single crystal X-ray diffraction were prepared by slow diffusion of pure hexanes into a solution of (**1**) in 3:1 carbon disulfide:hexanes to yield the solvate, $(\text{Ph}_3\text{P})_2\text{Pt}$ -MMK-9-*n*-hexane-methylcyclopentane.¹⁸ Crystals of a second solvate, $(\text{Ph}_3\text{P})_2\text{Pt}$ -MMK-9-3benzene, were

Department of Chemistry, University of California, Davis, California, USA.

E-mail: albalch@ucdavis.edu; Fax: +1 530 752 2820; Tel: +1 530 752 0941

† Electronic supplementary information (ESI) available: Synthetic and spectroscopic details and X-ray crystallographic files in CIF format for $(\text{Ph}_3\text{P})_2\text{Pt}$ -MMK-9 (**1**). CCDC 2087934 and 2087935. For ESI and crystallographic data in CIF or other electronic format see DOI: 10.1039/d1cc04336f



Scheme 1 Formation of $(\text{Ph}_3\text{P})_2\text{Pt-MMK-9}$ (**1**) by reaction of $(\text{Ph}_3\text{P})_4\text{Pt}$ with MMK-9 and the structure of MMK-15.

obtained by diffusion of pentane into a solution of $(\text{Ph}_3\text{P})_2\text{Pt-MMK-9}$ (**1**) in benzene.¹⁹ Both crystals show similar structures for the adduct $(\text{Ph}_3\text{P})_2\text{Pt-MMK-9}$ (**1**) with only small variations in the orientations of the phenyl rings. MMK-9 and the adduct obtained from it, $(\text{Ph}_3\text{P})_2\text{Pt-MMK-9}$ (**1**), are chiral molecules. However, $(\text{Ph}_3\text{P})_2\text{Pt-MMK-9}$ (**1**), like MMK-9 itself,¹⁶ crystallizes as a racemate in both solvates that were crystallized.

Fig. 1 shows the structure of the adduct $(\text{Ph}_3\text{P})_2\text{Pt-MMK-9}$ (**1**). The $(\text{Ph}_3\text{P})_2\text{Pt}$ unit has inserted into a C–C bond of MMK-9 that formerly connected C6 and C7 in the adduct (**1**). In MMK-9 the C6–C7 bond distance is 1.533(5) Å,¹⁴ but in $(\text{Ph}_3\text{P})_2\text{Pt-MMK-9}$ (**1**) the non-bonded separation between C6 and C7 is 2.59(1) Å. The Pt1–C6 bond length is 2.045(7) Å and the Pt1–C7 bond length is similar, 2.041(8) Å. For comparison, the Pt–C

bond lengths in $(\text{Ph}_3\text{P})_2\text{Pt}(\eta^1\text{-}\eta^1\text{-C}_6\text{H}_4\text{C}_6\text{C}_4)$ where the Pt–C bonds are trans to triphenylphosphine ligands are 2.068(5) and 2.092(5).²¹ While the C6–Pt–C7 angle, 78.8(3)°, is narrower than expected for a planar Pt(II) ion and the P1–Pt1–P2 angle, 99.73(7)°, is wider. The sum of the four angles involving the PtP_2C_2 unit is 360.13°, which is indicative of planar coordination about platinum. The bond distances and angles about the metal center in $(\text{Ph}_3\text{P})_2\text{Pt-MMK-9}$ when compared to a Pt adduct of semibuckminsterfullerene, which has C–Pt–C = 87.9(5)°, C–Pt = 2.055 Å, and C···C = 2.84 Å,¹⁵ indicate a lesser degree of ring strain in the open-cage ligand.

Fig. 2 shows a comparison of ring structure of the orifices in adduct $(\text{Ph}_3\text{P})_2\text{Pt-MMK-9}$ (**1**) at the top and MMK-9 below. The addition of the $(\text{Ph}_3\text{P})_2\text{Pt}$ unit has produced a bicyclic structure and opened the largest ring size to fifteen atoms, whereas MMK-9 contains a twelve-membered ring. Computations have shown that the LUMO in MMK-9 is localized in that portion of the rim adjacent to the C6–C7 bond.¹⁶ Thus, that portion of the molecule is set up to receive electrons from the platinum(0) center during oxidative addition, a factor that accounts for the regioselectivity of the insertion.

The insertion of the $(\text{Ph}_3\text{P})_2\text{Pt}$ unit into a C–C bond of MMK-9 contrasts markedly with the typical behavior of reactions of low valent metal complexes with empty-cage fullerenes: usually an adduct is formed at a 6:6 ring junction with the fullerene behaving similarly to an olefin.^{22,23} For example, the reaction of $(\text{Ph}_3\text{P})_2\text{Pt}(\eta^2\text{-C}_2\text{H}_4)$ with C_{60} produces $(\text{Ph}_3\text{P})_2\text{Pt}(\eta^2\text{-C}_{60})$, which contains the coordinating PtC_2 unit with Pt–C bond lengths of 2.145(24) and 2.115(23) Å, a C–C bond length of 1.502(30) Å, and a C–Pt–C angle of 41.3(8)°.²² Similarly, the reaction of $(\text{Ph}_3\text{P})_4\text{Pd}$ with several open-cage fullerenes produces adducts in which $(\text{Ph}_3\text{P})_2\text{Pd}$ units are attached to double bonds in η^2 -fashion along the rims of these open-cages.²⁴ In the present case, the insertion of the platinum has been facilitated by the curvature of the fullerene cage¹⁵ and the proximity of the activated C–C bond to the keto groups on the rim of the

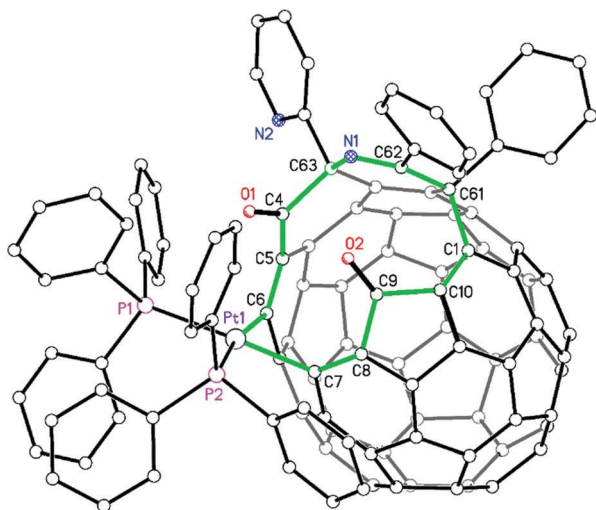


Fig. 1 Crystallographic structure of one enantiomer of the adduct $(\text{Ph}_3\text{P})_2\text{Pt-MMK-9}$ (**1**) obtained from a crystal of the solvate, $(\text{Ph}_3\text{P})_2\text{Pt-MMK-9}\cdot n$ -hexane-methylcyclopentane with the atoms shown as circles in order to simplify the drawing. The rim of the opening in the cage is shown with green bonds.

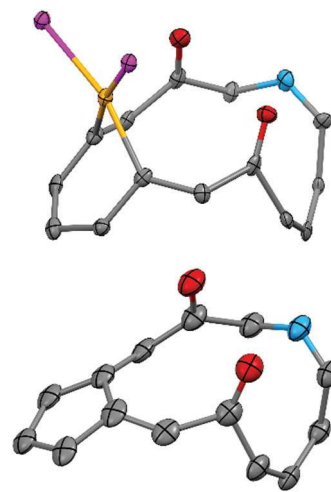


Fig. 2 Comparison of the orifices in adduct $(\text{Ph}_3\text{P})_2\text{Pt-MMK-9}$ (**1**)¹⁹ at the top and MMK-9 at the bottom. Color code: carbon, grey; nitrogen, blue; oxygen, red; platinum, yellow; phosphorus, pink.

opening. Placing a four-coordinate platinum ion within the rim still allows access to the interior of the cage and presents the opportunity to examine the behavior of a reactive metal center in this new type of open-cage fullerene. The adduct $(\text{Ph}_3\text{P})_2\text{Pt-MMK-9}$ provides a crystallographically characterized case in which a metal center becomes a part of the fabric of the fullerene framework. Such compounds may be useful as precursors to heterofullerenes. Previous work has detected the heterofullerenes, MC_{59}^+ and MC_{58}^+ , ($\text{M} = \text{Pt}$ or Ir) in which an M atom replaces one or two of the carbon atoms in the C_{60} cage.^{25,26} However, these species with metal atoms as part of the fullerene cage have only been observed in gas phase studies by mass spectrometry and have not been isolated in solid form.

The adduct $(\text{Ph}_3\text{P})_2\text{Pt-MMK-9}$ (**1**) is somewhat analogous to MMK-15, which is the product of sulfur insertion into MMK-9.¹⁶ In both cases it is the C6–C7 bond of MMK-9 that undergoes ring opening. However, the formation of MMK-15 requires harsher conditions involving heating a mixture of MMK-9, crown sulfur and tetrakis(dimethylamino)ethylene in refluxing *o*-dichlorobenzene.¹⁶ Structurally, $(\text{Ph}_3\text{P})_2\text{Pt-MMK-9}$ (**1**) and MMK-15 are similar. In both molecules, the C_5 portion of the PtC_5 or SC_5 ring is planar with the Pt or S atom protruding away from the fullerene surface. The distances between the two carbon atoms attached to Pt or S are similar: 2.596 Å for Pt and slightly shorter, 2.547 Å, for S .¹⁶

Electrochemical studies show that the adduct $(\text{Ph}_3\text{P})_2\text{Pt-MMK-9}$ (**1**) exhibits redox behavior that is found for other fullerenes. Fig. 3 compares the cyclic voltammograms for the first reduction process for $(\text{Ph}_3\text{P})_2\text{Pt-MMK-9}$ (**1**), MMK-9, and C_{60} . As the data show, $(\text{Ph}_3\text{P})_2\text{Pt-MMK-9}$ (**1**) does undergo a reduction, but at a potential that is much more negative than that found for either C_{60} or the more easily reduced MMK-9. A second, irreversible reduction wave is found at -2.02 V for $(\text{Ph}_3\text{P})_2\text{Pt-MMK-9}$ (**1**) while an irreversible oxidative wave is found at 0.83 V.

The UV/vis spectrum of $(\text{Ph}_3\text{P})_2\text{Pt-MMK-9}$ (**1**) shows features typical of other open-cage modifications of C_{60} .¹⁶ Fig. 4 shows a comparison of the UV/vis spectra of MMK-9 and $(\text{Ph}_3\text{P})_2\text{Pt-MMK-9}$ (**1**). The latter shows absorption shoulder at 570 nm,

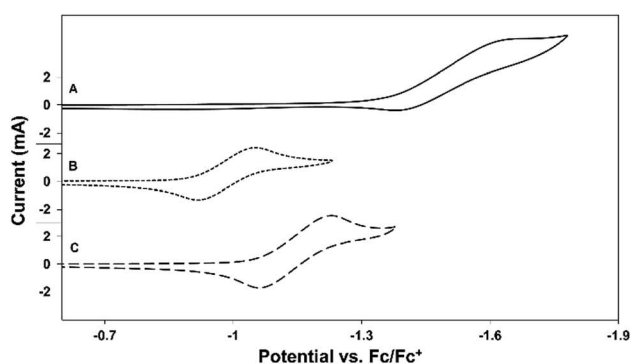


Fig. 3 Cyclic voltammograms of A, $(\text{Ph}_3\text{P})_2\text{Pt-MMK-9}$ (**1**); B, MMK-9; C, C_{60} using 1.0 mM solutions in *o*-dichlorobenzene solution with 50 mM tetra(*n*-butyl)ammonium hexafluorophosphate as supporting electrolyte at a scan rate of 0.01 V s^{-1} with a glassy carbon working electrode.

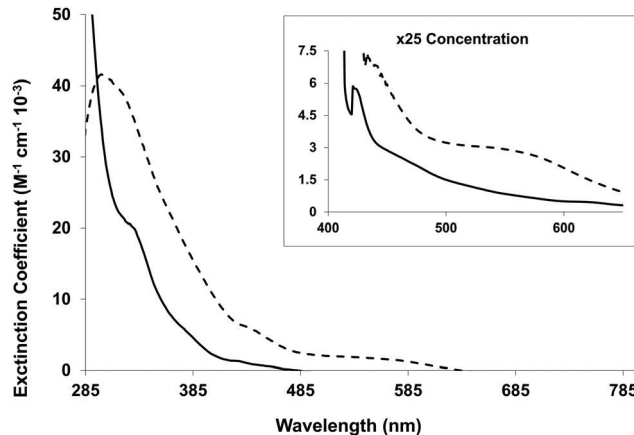


Fig. 4 UV/vis spectra of MMK-9 (solid line) and $(\text{Ph}_3\text{P})_2\text{Pt-MMK-9}$ (**1**) (dotted line) taken in 0.025 mM solution.

which is responsible for the darker color of solution of the platinum adduct. The infrared spectrum of $(\text{Ph}_3\text{P})_2\text{Pt-MMK-9}$ (**1**) exhibits two carbonyl absorptions at 1685 and 1731 cm^{-1} , whereas the parent MMK-9 has two corresponding absorptions at 1700 and 1744 cm^{-1} (see the ESI†). Thus, insertion of the platinum atom into the cage lowers the carbonyl stretching frequencies, which is a general consequence of increasing the ring size of cyclic ketones.²⁷

The insertion of a $(\text{Ph}_3\text{P})_2\text{Pt}$ unit into a carbon–carbon bond of MMK-9 as shown in Scheme 1 occurs under unusually mild conditions. Activation and cleavage of carbon–carbon bonds is generally restricted to strained situations as found in three- and four-membered rings.^{28,29} Here, the insertion occurs into a carbon–carbon bond (one of many such carbon–carbon bonds in this open-cage fullerene) in a five-membered ring. The platinum bonding to the open-cage fullerene is quite robust with the complex surviving chromatographic separation and aerobic handling in both solution and crystalline form. In contrast, many transition metal adducts of fullerenes are quite labile.²³ In forming $(\text{Ph}_3\text{P})_2\text{Pt-MMK-9}$ (**1**), it is likely that the $(\text{Ph}_3\text{P})_2\text{Pt}$ group initially coordinated to one of the C–C double bonds adjacent to the C6–C7 bond and then underwent oxidative addition to cleave the C6–C7 bond. This process resulted in the formation of a planar, 16 electron platinum(II) complex with a d^8 electron configuration. While the precursor $\text{Pt}(0)$ complex is rather labile in regard to ligand loss and gain, planar platinum(II) complexes are inert. The stability of the planar platinum(II) center coupled with the ring expansion that occurs upon adduct formation accounts for the robust nature of $(\text{Ph}_3\text{P})_2\text{Pt-MMK-9}$ (**1**).

The reactivity of open-cage fullerenes with metal complexes has shown some remarkable transformations. For MMK-9, these reactions include the insertion of a $(\text{Ph}_3\text{P})_2\text{Pt}$ unit into a carbon–carbon bond reported here, the addition of five methoxy groups in the presence of silver ion, methanol and dioxygen,¹⁷ and the formation of a carbon–carbon bond by coupling of two carbonyl groups as seen in the reaction of MMK-9 with triruthenium dodecacarbonyl.¹⁴ Detailed

understanding of the processes by which metal atoms become coordinated to the *rim* of open-cage fullerenes is crucial to developing a methodology for introducing metal atoms to the *inside* of open-cage fullerenes or as part of a heterofullerene.

We thank the National Science Foundation (Grant CHE-1807637) for support of this project.

Conflicts of interest

There are no conflicts to declare.

Notes and references

- 1 A. Hirsch and M. Brettreich, *Fullerenes: Chemistry and Reactions*, Wiley-VCH, New York, 2005.
- 2 K. Komatsu, M. Murata and Y. Murata, *Science*, 2005, **307**, 238–240.
- 3 K. Kurotobi and Y. Murata, *Science*, 2011, **333**, 613–616.
- 4 A. Krachmalnicoff, R. Richard Bounds, S. Mamone, S. Alom, M. Concistrè, B. Meier, K. Kouril, M. E. Light, M. R. Johnson, S. Rols, A. J. Horsewill, A. Shugai, U. Nagel, T. Rööm, M. Carravetta, M. H. Levitt and R. J. Whitby, *Nat. Chem.*, 2016, **8**, 953–957.
- 5 G. C. Vougioukalakis, R. Roubelakis and M. Orfanopoulos, *Chem. Soc. Rev.*, 2010, **39**, 817–844.
- 6 C. S. Chen, T. S. Kuo and W. Y. Yeh, *Chem. – Eur. J.*, 2016, **22**, 8773–8776.
- 7 W. Krätschmer, L. D. Lamb, K. Fostiropoulos and D. R. Huffman, *Nature*, 1990, **347**, 354–358.
- 8 A. A. Popov, S.-F. Yang and L. Dunsch, Endohedral fullerenes, *Chem. Rev.*, 2013, **113**, 5989–6113.
- 9 A. Rodriguez-Forteza, A. L. Balch and J. M. Poblet, *Chem. Soc. Rev.*, 2011, **40**, 3551–3563.
- 10 M. Mikawa, H. Kato, M. Okumura, M. Narazaki, Y. Kanazawa, N. Miwa and H. Shinohara, *Bioconjugate Chem.*, 2001, **12**, 510–514.
- 11 K. B. Ghiassi, M. M. Olmstead and A. L. Balch, *Dalton Trans.*, 2014, **43**, 7346–7358.
- 12 T. Li and H. C. Dorn, *Small*, 2017, **13**, 1603152.
- 13 Z. Zhou, N. Xin and L. Gan, *Chem. – Eur. J.*, 2018, **24**, 451–457.
- 14 C.-S. Chen, Y.-F. Lin and W.-Y. Yeh, *Chem. – Eur. J.*, 2014, **20**, 936–940.
- 15 C. M. Alvarez, R. J. Angelici, A. Sygula, R. Sygula and P. W. Rabideau, *Organometallics*, 2003, **22**, 624–626.
- 16 Y. Murata, M. Murata and K. Komatsu, *Chem. – Eur. J.*, 2003, **9**, 1600–1609.
- 17 A. Aghabali, S. Jun, M. M. Olmstead and A. L. Balch, *J. Am. Chem. Soc.*, 2016, **138**, 16459–16465.
- 18 Crystal data for $(\text{Ph}_3\text{P})_2\text{Pt-MMK-9-}n$ -hexane-methylcyclopentane. $\text{C}_{116}\text{H}_{44}\text{N}_2\text{O}_2\text{P}_2\text{Pt}\cdot\text{C}_6\text{H}_{14}\cdot\text{C}_6\text{H}_{12}$: $M = 1924.89$, dark red plate $0.420 \times 0.270 \times 0.150$ mm, $\lambda = 71073$ Å, ApexII CCD, triclinic, space group $P\bar{1}$ (no. 2), $a = 14.8879(4)$, $b = 16.0972(4)$, $c = 19.9238(6)$ Å, $\alpha = 79.1823(16)$, $\beta = 80.6461(16)$, $\gamma = 65.3053(14)^\circ$, $T = 90(2)$ K, $V = 4242.1(2)$ Å³, $Z = 2$, 16 695 reflections measured, 16 695 unique ($R_{\text{int}} = 0.0899$) which were used in all calculations, $2\theta_{\text{max}} = 52.082^\circ$; min/max transmission = 0.526/0.779 (multi-scan absorption correction applied); direct and Patterson methods solution; full-matrix least squares based on F_2 (SIR2004 and SHELXL-2018); the final $wR(F_2)$ was 0.1827 (all data), conventional $R_1 = 0.0733$ computed for 16695 reflections with $I > 2\sigma(I)$ using 1184 parameters with 13 restraints.
- 19 Crystal data for $(\text{Ph}_3\text{P})_2\text{Pt-MMK-9-3benzene}$. $\text{C}_{116}\text{H}_{44}\text{N}_2\text{O}_2\text{P}_2\text{Pt}\cdot 3\text{C}_6\text{H}_6$ $M = 1988.88$, red plate $0.0214 \times 0.149 \times 0.082$ mm, $\lambda = 0.71703$ Å, Bruker Kappa Duo, space group $P\bar{1}$ (no. 2), $a = 14.7186(12)$, $b = 16.4565(14)$, $c = 19.6359(16)$ Å, $\alpha = 79.689(2)$, $\beta = 81.529(2)$, $\gamma = 65.546(2)^\circ$, $T = 100(2)$ K, $V = 4245.3(6)$ Å³, $Z = 2$, 17 544 reflections measured, 17 544 unique ($R_{\text{int}} = 0.1214$) which were used in all calculations, $2\theta_{\text{max}} = 53.64^\circ$; min/max transmission = 0.677, 0.745, multi-scan absorption correction applied; direct and Patterson methods solution; full-matrix least squares based on F_2 (SIR2004 and SHELXL-2018); the final $wR(F_2)$ was 0.1451 (all data), conventional $R_1 = 0.0582$ computed for 14 022 reflections with $I > 2\sigma(I)$ using 1265 parameters with 558 restraints.
- 20 A. Sen and J. Halpern, *Inorg. Chem.*, 1980, 1073–1075.
- 21 M. A. Bennett, T. Dirnberger, D. C. R. Hockless, E. Wenger and A. C. Willis, *Dalton Trans.*, 1998, 271–278.
- 22 P. J. Fagan, J. C. Calabrese and B. Malone, *Science*, 1991, **252**, 1160–1161.
- 23 A. L. Balch and M. M. Olmstead, *Chem. Rev.*, 1998, **98**, 2123–2165.
- 24 H. Zhang, Z. Zhou, L. Yang, J. Su, P. Jin and L. Gan, *Organometallics*, 2019, **38**, 3139–3143.
- 25 J. M. Poblet, K. Winkler, M. Cancilla, A. Hayashi, C. B. Lebrilla and A. L. Balch, *Chem. Commun.*, 1999, 493–494.
- 26 A. Hayashi, Y. Xie, J. M. Poblet, J. M. Campanera, C. B. Lebrilla and A. L. Balch, *J. Phys. Chem. A*, 2004, **108**, 2192–2198.
- 27 J. I. Brauman and V. W. Laurie, *Tetrahedron*, 1968, **24**, 2595–2601.
- 28 Y. Cohen, A. Cohen and I. Marek, *Chem. Rev.*, 2021, **121**, 140–161.
- 29 M. Murakami and N. Ishida, *Chem. Rev.*, 2021, **121**, 264–299.